Published in final edited form as:
Nat Med. 2013 June ; 19(6): 760–765. doi:10.1038/nm.3185.

Semaphorin 3d signaling defects are associated with anomalous pulmonary venous connections

Karl Degenhardt[1,9], **Manvendra K Singh**[2,3,4,9], **Haig Aghajanian**[2,3,4,9], **Daniele Massera**[2,3,4], **Qiaohong Wang**[2,3,4], **Jun Li**[2,3,4], **Li Li**[2,3,4], **Connie Choi**[2,3,4], **Amanda D Yzaguirre**[2,5], **Lauren J Francey**[6], **Emily Gallant**[6], **Ian D Krantz**[6], **Peter J Gruber**[7,8], and **Jonathan A Epstein**[2,3,4]

[1]Department of Pediatrics, Division of Cardiology, Children's Hospital of Philadelphia, Perelman School of Medicine at the University of Pennsylvania, Philadelphia, Pennsylvania, USA.

[2]Department of Cell and Developmental Biology, Perelman School of Medicine at the University of Pennsylvania, Philadelphia, Pennsylvania, USA.

[3]Cardiovascular Institute, Perelman School of Medicine at the University of Pennsylvania, Philadelphia, Pennsylvania, USA.

[4]Institute for Regenerative Medicine, Perelman School of Medicine at the University of Pennsylvania, Philadelphia, Pennsylvania, USA.

[5]Abramson Family Cancer Research Institute, Perelman School of Medicine at the University of Pennsylvania, Philadelphia, Pennsylvania, USA.

[6]Department of Pediatrics, Division of Human Genetics, Children's Hospital of Philadelphia, Perelman School of Medicine at the University of Pennsylvania, Philadelphia, Pennsylvania, USA.

[7]Department of Surgery, University of Utah School of Medicine, Salt Lake City, Utah, USA.

[8]Department of Molecular Medicine, University of Utah School of Medicine, Salt Lake City, Utah, USA.

Abstract

Total anomalous pulmonary venous connection (TAPVC) is a potentially lethal congenital disorder that occurs when the pulmonary veins do not connect normally to the left atrium, allowing mixing of pulmonary and systemic blood[1]. In contrast to the extensive knowledge of arterial vascular patterning, little is known about the patterning of veins. Here we show that the secreted guidance molecule semaphorin 3d (Sema3d) is crucial for the normal patterning of pulmonary veins. Prevailing models suggest that TAPVC occurs when the midpharyngeal endothelial strand (MES), the precursor of the common pulmonary vein, does not form at the proper location on the dorsal surface of the embryonic common atrium[2,3]. However, we found that TAPVC occurs in Sema3d mutant mice despite normal formation of the MES. In these embryos, the maturing pulmonary venous plexus does not anastomose uniquely with the properly formed

Correspondence should be addressed to J.A.E. (epsteinj@upenn.edu)..
[9]These authors contributed equally to this work.

AUTHOR CONTRIBUTIONS

K.D., M.K.S., H.A. and J.A.E. performed project planning, experimental work, data interpretation and preparation of the manuscript. D.M., Q.W., J.L., L.L., C.C. and A.D.Y. performed experimental work. L.J.F., E.G., I.D.K. and P.J.G. participated in the identification of *SEMA3D* variants. J.A.E. supervised all aspects of the research.

Note: Supplementary information is available in the online version of the paper.

COMPETING FINANCIAL INTERESTS

The authors declare no competing financial interests.

MES. In the absence of Sema3d, endothelial tubes form in a region that is normally avascular, resulting in aberrant connections. Normally, Sema3d provides a repulsive cue to endothelial cells in this area, establishing a boundary. Sequencing of *SEMA3D* in individuals with anomalous pulmonary veins identified a phenylalanine-to-leucine substitution that adversely affects SEMA3D function. These results identify Sema3d as a crucial pulmonary venous patterning cue and provide experimental evidence for an alternate developmental model to explain abnormal pulmonary venous connections.

Complete separation of the systemic and pulmonary circulations occurs shortly after birth in humans. In adults, the right ventricle pumps blood through the pulmonary arteries to the lungs, and oxygenated blood returns to the left atrium through the pulmonary veins. The left ventricle pumps blood to the systemic circulation, where oxygen is used by peripheral tissues, and deoxygenated blood is returned through the systemic veins to the right atrium. Improper connection of some or all of the pulmonary veins to the right atrium or systemic venous system is termed partial anomalous pulmonary venous connection (PAPVC) and TAPVC, respectively[1,3,4]. The end result is a left-to-right shunt that can lead to cyanosis, increased volume load on the right heart and heart failure. PAPVC has been reported in up to 1 in 140 individuals (0.7%)[5–8]. TAPVC is less common but can result in severe cyanosis or congestive heart failure in infants. Left untreated, the mortality of TAPVC is 80%[9].

In contrast to our progress in understanding the morphogenesis of the cardiac outflow tracts and great arteries, little is known about the molecular regulation of pulmonary vein formation. Early development of the pulmonary veins is similar among vertebrate species, including humans[10]; subtle differences become evident at later stages. For example, in humans the pulmonary vein is incorporated into the back wall of the left atrium, and subsequent remodeling leaves four separate orifices[11], whereas in mice there is a single common pulmonary vein that enters the left atrium. Descriptive anatomical studies have suggested that pulmonary veins form initially as a dorsal evagination from the posterior wall of the embryonic atrium[10], leading researchers to speculate that abnormal venous connections arise from absent or mislocalized evaginations[2,3]. According to this model, TAPVC is caused primarily by defects in the formation or maintenance of the MES, which is the anlage of the pulmonary veins[12–15]. Recently, high-resolution three-dimensional reconstructions of avian embryos have helped clarify that the pulmonary vein derives from a greater vascular plexus within the splanchnic mesoderm[16]. Incomplete remodeling of this plexus with failure of separation into distinct pulmonary and systemic vascular zones has been postulated to be a developmental defect that could result in anomalous pulmonary venous connection[16].

Human genetic studies of kindreds with TAPVC have provided evidence for autosomal-dominant inheritance with incomplete penetrance and variable expression[17,18], and genetic linkage analysis has implicated loci on human chromosome 4q12 (ref. 18). Candidate genes in this region include the gene encoding vascular endothelial growth factor receptor 2 (*KDR*) and the gene encoding platelet-derived growth factor receptor α (*PDGFRA*). Indeed, a spectrum of inflow tract defects, including a low incidence of TAPVC, has been noted in mice after inactivation of *Pdgfra* either globally or in the dorsal mesocardium[19]. Overexpression of the *ANKRD1* gene is also associated with TAPVC, as shown through a chromosomal translocation in one individual and a mutation in a putative PEST (ProGluSerThr) degradation motif in two affected siblings[20]. The molecular mechanisms by which perturbations in these genes might lead to anomalous connection of the pulmonary veins has yet to be described.

Class 3 semaphorins are secreted molecules that signal primarily through the neuropilin, plexin or both co-receptor complexes. Semaphorins were originally identified as axon

guidance molecules but have since been implicated in multiple biological processes, including cardiovascular patterning[21–23]. For example, *Sema3e* is required for intersomitic artery patterning[24], and *Sema3c* is required for morphogenesis of the great arteries at the arterial pole of the heart[25]. *Sema3d* encodes a related member of this class of proteins that has been previously implicated in retinal ganglion cell axon patterning and neural crest migration in zebrafish[26,27].

To determine the role of *Sema3d* in cardiovascular development, we inactivated the gene by homologous recombination in mouse embryonic stem cells (**Supplementary Fig. 1** and ref. 28). We created two distinct alleles: one resulted in truncation of the protein after the seventh amino acid residue, and in the other the coding sequence for a fusion of GFP and Cre recombinase was inserted at the initiating ATG codon. GFP expression from this allele accurately recapitulates endogenous *Sema3d* expression[28]. The resulting phenotypes of the two alleles were identical (data not shown). Heterozygous mice appeared normal, whereas homozygous-null mice showed abnormalities of pulmonary venous patterning. Affected *Sema3d*$^{-/-}$ adult mice had massively enlarged right atria and ventricles (**Fig. 1** and **Supplementary Video 1**), consistent with a left-to-right shunt. In control mice (either wild type or *Sema3d*$^{+/-}$), the pulmonary veins connected to the left atrium (**Fig. 1a,c,e,f**). The mutant mice had anomalous connections to the coronary sinus (which connects to the right atrium) or directly to the right atrium (**Fig. 1b,d,g,h, Supplementary Video 2** and **Supplementary Fig. 2**). Thirty-five percent (14/36) of homozygous-null mutants had TAPVC or PAPVC. The majority of the affected mice had TAPVC (13/14). TAPVC was associated with atrial septal defects in all affected *Sema3d* mutants. However, we did not note any other structural intracardiac defects or abnormalities of laterality in the abdominal organs of the mutant mice.

To determine when patterning defects were first evident, we examined *Sema3d*$^{-/-}$ mouse embryos at progressively earlier stages. At embryonic day (E) 17.5, optical projection tomography (OPT) imaging (**Fig. 2a,b**) identified examples of abnormal connections of the pulmonary vein to the coronary sinus (3 of 8 mutant embryos) (**Fig. 2b**). At E12.5 (**Fig. 2c,d** and **Supplementary Video 3**), there were also abnormal pulmonary venous connections in some (4 of 11) *Sema3d* mutant embryos (**Fig. 2d**). Staining for expression of the endothelial marker Pecam1 at E10.5 (**Fig. 2e,f**) revealed the first signs of abnormalities of vascular patterning in the region of the nascent pulmonary veins in some (4 of 10) mutant embryos, suggesting the formation of abnormal venous connections in ectopic locations (**Fig. 2f**). At E9.5, there were no abnormalities in endothelial patterning (**Fig. 2g,h** and **Supplementary Fig. 3**). Notably, the MES was easily identifiable at E9.5 and was unperturbed in *Sema3d*$^{-/-}$ embryos (0 of 9 mutant embryos) (**Fig. 2g,h** and **Supplementary Fig. 3**). This finding contradicts the widely held belief that failure of normal pulmonary vein formation at the site of entry to the common atrium is the primary defect leading to TAPVC[15,20]. Rather, our findings suggest that the patterning and connections of the pulmonary portion of the splanchnic venous plexus may be disrupted.

Class 3 semaphorins signal through receptor complexes containing neuropilins[29]. We examined Sema3d expression as marked by GFP immunofluorescence in *Sema3d*$^{GFPCre/+}$ mice and neuropilin-1 (Nrp-1) expression by immunofluorescence (**Fig. 3**). At E10.5, when patterning defects were first present, Sema3d was expressed in the mesocardial reflections that form an anatomic boundary between the splanchnic mesoderm and the venous pole of the heart (**Fig. 3a–c,h,i**). Nrp-1 was expressed by the MES at E9.5 and by pulmonary endothelial cells during early pulmonary vein patterning (**Fig. 3d,e** and **Supplementary Fig. 4**). Nrp-1 has been reported to be arterial specific in the chick[30], although not in other systems[31,32]. We performed double staining for Nrp-1 and Eph receptor B4 (EphB4), a

marker of venous endothelium, and found that Nrp-1 and EphB4 were coexpressed on pulmonary venous endothelium (**Fig. 3e,f**).

To determine whether Sema3d binds to the pulmonary vein endothelium *in vivo*, we incubated cryosections from wild-type E10.5 embryos with conditioned medium from HEK293T cells expressing alkaline phosphatase–tagged Sema3d (Sema3d-AP) protein. We detected Sema3d-AP binding in the region of the nascent pulmonary veins (**Fig. 3g**) but found no alkaline phosphatase binding on sections treated with control conditioned medium (data not shown). The pulmonary venous plexus is normally constrained entirely to the region medial to the Sema3d expression domain and anastomoses with the MES (**Fig. 3h**). However, in *Sema3d* mutants, numerous Pecam1-positive endothelial cells and tubes penetrate the lateral and caudal boundaries and intermingle with cells that would normally express Sema3d (identified by GFP immunohistochemistry in mutant specimens) (**Fig. 3i**). Quantification of serial confocal stacks confirmed significantly greater overlap of GFP and Pecam1 expression in mutants compared to controls (**Fig. 3j**). Sema3d deficiency did not affect pulmonary endothelial cell proliferation or survival (**Supplementary Fig. 5**), suggesting that Sema3d regulates pulmonary vein patterning by directing pulmonary endothelial cell localization.

Previous work identified an avascular zone that forms within the splanchnic plexus to separate the pulmonary venous plexus from the more caudal vascular structures associated with systemic veins[16]. Notably, Sema3d was expressed specifically within this avascular zone (**Supplementary Fig. 6a–g**), and this domain of Sema3d expression was inappropriately vascularized in *Sema3d* mutants (**Supplementary Fig. 6h–k**). These findings are consistent with the hypothesis that the failure of this avascular region to form could result in abnormal connections, as previously postulated[16].

Given these findings in mice, we examined humans with APVC for possible pathogenic variants in *SEMA3D*. We sequenced the exons of *SEMA3D* in 40 individuals with anomalous pulmonary venous connections (19 individuals with TAPVC and 21 individual with PAPVC) and identified several variants (**Supplementary Table 1**). We found one of these variants, a c.193T>C missense mutation that results in a serine-to-proline substitution (S65P), in both the affected and control populations at approximately equal frequencies (1/20). However, a second variant, a c.1806T>A missense mutation that results in a phenylalanine-to-leucine substitution (F602L), was present only in an individual with PAVPC and not in 80 control samples (**Supplementary Table 1** and **Supplementary Fig. 7**). The affected individual was of European ancestry (as were 78 of 80 controls), had PAPVC with an associated ventricular septal defect and had no evidence of heterotaxy syndrome. The pattern of inheritance for this mutation could not be determined, as parental DNA was not available for this individual. The F602L variant is predicted to be possibly damaging to protein function by PolyPhen *in silico* analysis (**Supplementary Table 1**), and the amino acid alteration is located in the immunoglobulin-like domain of Sema3d, which has been shown to be important for both receptor binding and functional activity[33,34]. Additionally, the F602L variant is absent from the 1000 Genomes data set (1,092 individuals) and the National Heart, Lung, and Blood Institute Exome Sequencing Project (ESP) (13,000 chromosomes)[35] and is not among the >800 chromosomes reported previously in which *SEMA3D* exons were sequenced for other reasons[36,37].

To test the ability of wild-type and variant Sema3d to bind to neuropilin receptors and mediate the guidance of endothelial cells, we generated alkaline phosphatase fusion proteins. Binding to transfected COS-7 cells expressing Nrp-1 or Nrp-2 suggested that wild-type and both Sema3d variants tested could bind to Nrp-1, although the F602L variant bound with lower affinity (**Fig. 4a** and **Supplementary Fig. 8**). We found no substantial binding to

Nrp-2. Wild-type Sema3d-AP bound to human umbilical vein endothelial cells (HUVECs) (**Supplementary Fig. 9**), which normally express NRP-1 (refs. 31,32). This binding was significantly ($P < 0.001$) diminished after siRNA-mediated knockdown of NRP-1 expression (**Supplementary Fig. 10**).

To determine the endothelial guidance properties of Sema3d variants, we cocultured HEK293 cells overexpressing either Sema3d or its variants with HUVECs. Time-lapse video analysis, as well as micrograph quantification, confirmed that Sema3d acts as a migratory repulsive cue in culture[21] (**Fig. 4b,c** and **Supplementary Video 4**). The Sema3d S65P variant repelled HUVECs similarly to the wild-type protein (**Fig. 4b,c**); however, the Sema3d F602L variant had markedly reduced repulsion activity (**Fig. 4b,c** and **Supplementary Video 4**). To investigate whether Sema3d repulsion is mediated by NRP-1, we blocked NRP-1 signaling by adding either soluble NRP-1 or an NRP-1–specific blocking antibody to the culture medium. Both soluble NRP-1 and the NRP-1–specific antibody significantly reduced HUVEC repulsion in response to Sema3d (**Fig. 4d,e**).

Although both arterial and venous endothelia express Nrp-1, recent studies have shown that cell responsiveness to semaphorin signaling can be mediated by differential expression of co-receptors, as well as intracellular signaling factors acting downstream of receptors[38,39]. For example, Sema3e acts as a repellent signal on neurons expressing plexin D1 but not Nrp-1 and acts as an attractive cue for neurons that express both proteins[38]. Recently, the effects of Sema3f in the central nervous system were shown to be modulated by an intra-cellular Rac GTPase-activating protein, β2-chimaerin (β2Chn)[39]. In the absence of β2Chn, Sema3f engagement of Nrp-2 can mediate axon repulsion, but β2Chn is required for axon pruning in response to Sema3f. Thus, the downstream effects of semaphorin-neuropilin interactions may be dictated by the expression or activities of receptors and downstream mediators.

Taken together these data implicate Sema3d as a repellent guidance molecule that functions to pattern the forming pulmonary venous vasculature (**Fig. 4f**). We suggest that in the absence of Sema3d-mediated repulsion, the pulmonary vasculature stochastically forms anomalous connections to adjacent systemic venous structures along a broad rostral-caudal domain, which could explain the morphological variability of anomalous pulmonary vascular connections in *Sema3d* mutant mice and the diverse types of anomalous connections in affected humans[16]. The lack of repulsion leads to a broad domain of abnormal endothelial sprouts, which may persist when they connect to a systemic vein and receive substantial blood flow. Hence, stochastic considerations may contribute to variation in patterning.

SEMA3D copy number variation has been linked to congenital heart defects[40], and the functional deficiencies of the F602L variant suggest a possible genetic contribution to this common form of congenital heart disease in children, although further studies will be necessary to determine whether *SEMA3D* mutations are sufficient to cause APVC in humans and to what degree sequence variation in *SEMA3D* may contribute to this phenotype. Genetic variation affecting the SEMA3D signaling cascade will be an important future target of study in individuals with congenital heart disease and pulmonary venous anomalies.

Our data demonstrate a new pathophysiological mechanism for anomalous pulmonary venous connections that challenges the long-held model regarding the etiology of this congenital disorder. These findings underscore the existence of specific morphogenetic pathways affecting subtypes of the vasculature and the importance of further investigation into the nature of vascular heterogeneity in development and disease.

ONLINE METHODS

Generation of *Sema3d* mutant mice

All animal experiments were performed under University of Pennsylvania Institutional Animal Care and Use Committee–approved protocols. The generation and genotyping of *Sema3d*^{GFPCre} knock-in mice are described elsewhere[41]. *Sema3d*$^{+/-}$ mice were made in a similar manner: ~20 kb of mouse genomic sequence surrounding exon 2 of the *Sema3d* gene (chromosome 5: 12438103–12457989 of the NCBI37/mm9 assembly) was recombineered into the pL253 plasmid[41]. A FRTed PGKneo cassette was recombineered into exon 2, removing the splice donor of exon 2. The recombineering also placed stop codons 18 bp downstream of the ATG start codon (**Supplementary Fig. 1**). Correctly targeted TL-1 embryonic stem cells were identified by PCR. The primers used for screening were Sema3d forward, 5′-ATGACTGGGCACAACAGACAATCGG-3′ and Sema3d reverse, 5′-TGAGGATGGGAACTGGTGGTATCAG-3′ (**Supplementary Fig. 1b**). Targeting was also confirmed by Southern blotting (digestion with EcoRV followed by hybridization with a probe corresponding to chromosome 5: 12436819–12437431; the wild-type band is ~22 kb in size and the mutant band ~12 kb in size) (**Supplementary Fig. 1c**). After blastocyst injection, germline transmission from chimeric males was confirmed by Southern blotting and PCR as described above and the mutant allele was followed in subsequent generations by PCR with the following primers: forward, 5′-ATTGCATCGCATTGTCTGAG-3′ (F1) and reverse, 5′-CTGCCACTGTCCTTCATTCC-3′ (R1). *Sema3d*$^{neo/+}$ mice (harboring the neomycin cassette) were crossed to β-actin FLPe mice (Jackson Labs) to remove the neomycin cassette, generating *Sema3d*$^{+/-}$ mice. Confirmation of FLPe-mediated excision of the cassette was performed by PCR using the forward primer 5′-GAATGTTACTAAAGATAGCTAACTGACG-3′ (F2) and the reverse primer 5′-CTGCCACTGTCCTTCATTCC-3′ (R1) (**Supplementary Fig. 1d,e**). *Sema3d* expression in adult (2 months old) tissue was analyzed using the forward primer 5′-TGCTAGCAGGAAGGGTGAAC-3′ and the reverse primer 5′-TAGGTTAGCTTGAGTCTTGG-3′ (**Supplementary Fig. 1f**).

Both *Sema3d*^{GFPCre} and *Sema3d*$^{-}$ alleles are considered null and referred to as *Sema3d*$^{-}$ for analysis of the phenotype. The *Sema3d*^{GFPCre} allele is specified in experiments that make use of the GFP reporter. *Sema3d* controls (either wild type or *Sema3d*$^{+/-}$) and mutant embryos on a mixed Sv129 and C57BL/6 genetic background were analyzed at various developmental stages for APVC (8 control and 8 mutant mice at E16.5–E17.5 (3 of 8 mutants were affected), 16 control and 11 mutants at E11.5–E12.5 (4 of 11 mutants were affected), 11 control and 10 mutants at E10.5 (4 of 10 mutants were affected) and 10 control and 9 mutants at E9.5 (0 of 9 mutants were affected)).

MicroCT

MicroCT of iodine-stained mouse tissue was performed as described[42]. Briefly, tissue was fixed in 4% paraformaldehyde. After fixation, tissue was washed in PBS and stained in 25% Lugol's solution before scanning. Reconstructed data sets were viewed in OsiriX (http://www.osirix-viewer.com) for creating figures and movies.

OPT

OPT was performed on both unstained and whole-mount immunostained embryos using a Bioptonics OPT Scanner 3001M according to the manufacturer's instructions. Briefly, whole-mount immunostained embryos were embedded in agarose and dehydrated in methanol before clearing in benzyl alcohol–benzobenzoate (BABB) for scanning. Reconstructed data sets were viewed in OsiriX for creating figures and movies.

Immunohistochemistry

Embryos were dissected in PBS and fixed immediately in 4% paraformaldehyde for 16–20 h at 4 °C. Samples were washed with PBS, dehydrated in a methanol series and stored in 100% methanol at –20 °C. Immunofluorescent detection of GFP (Abcam, AB6673, 1:100), Pecam1 (Pharmingen, 553370, 1:500), EphB4 (R&D Systems, AF446, 1:100), phosphorylated histone H3 (Cell Signaling, 9706, 1:200) and Nrp-1 (Abcam, AB81321, 1:100) was performed on paraffin sections of paraformaldehyde-fixed embryos. TUNEL staining was performed using *In Situ* Cell Death Detection Kit Fluorescein from Roche Boehringer Mannheim (11684795910). Whole-mount immunofluorescence studies of *Sema3d*$^{GFPCre/+}$ and *Sema3d*$^{GFPCre/GFPCre}$ embryos for Pecam1 and GFP were carried out as described[43,44]. Quantification of cells staining for both Pecam1 and GFP was done with ImageJ (imagej.nih.gov/ij) on stacks of confocal images. The 'auto' setting was used for setting the threshold of the green channel (GFP) to make a mask extending approximately 10 μm around each labeled nucleus. The mask was then placed on the red (Pecam1) channel, and measurements of integrated density of pixels were taken.

Alkaline phosphatase binding assay

The mouse *Sema3d* coding sequence was cloned into the pAPtag5 plasmid[45] and transfected into HEK293T cells to produce conditioned medium. Wild-type and variant forms of Sema3d-AP were expressed and secreted at similar levels (data not shown). Binding to transfected (with empty vector, Nrp-1 or Nrp-2) COS-7 cells was performed as described[46]. To ensure equivalent amounts of Nrp-1 and Nrp-2 expression, COS-7 cells were first transfected and then passaged into multiple wells before exposure to Sema3d-AP ligands. Equal molar ratios (as calculated from alkaline phosphatase enzymatic activity) of the Sema3d-AP variants were incubated with transfected cells. Sema3d-AP protein binding to tissue sections was performed as previously described[47]. Control (AM4611) and *Nrp-1* (AM16704) siRNA were purchased from Ambion. HUVECs were transfected with either control or *Nrp-1* siRNA (200 nM) using RNAiMAX (Invitrogen, 13778030) for 48 h before Sema3d-AP binding. Nrp-1 knockdown was confirmed by quantitative RT-PCR using Nrp-1 forward (5′-TATTCCCAGAACTCTGCCC-3′) and reverse (5′-TGTCATCCACAGCAATCCCA-3′) primers. Nrp-2 was used as a control, with the forward primer 5′-CCTGTGGTTGGATGTATGAC-3′ and the reverse primer 5′-GCAGTTCTCCAGTGGGACAT-3′. All expression values were normalized to β-actin.

Endothelial cell repulsion assays

HUVECs (lot #1023) and culture medium (Vasculife EnGS Complete Kit, LL-0002) were purchased from Lifeline Cell Technology and cultured according to the instructions of the manufacturer. To generate virus, HEK293T cells in 10-cm cell culture plates were transiently transfected with pLOVE (Addgene) constructs containing coding sequence for Sema3d variants, pLOVE-Sema3d (wild type), pLOVE-Sema3d (S65P), pLOVESema3d (F602L) or GFP in addition to packaging plasmids pMD.G and psPAX2 (Addgene) using the FuGene transfection reagent. Lentiviral particles were collected after 24 and 48 h and concentrated using Millipore centrifugal filter units. The presence of virus was confirmed with Clontech instant lentiviral titer tests. HEK293 cells in 6-cm cell culture plates were subsequently infected with the harvested virus for 48 h. After 48 h, the infected cells were resuspended in medium, washed, incubated with DiI solution and plated on top of ~75% confluent HUVECs. The mixture of cells was incubated for 24 h and observed with a Nikon Eclipse TE200 inverted microscope under a ×20 objective. For Nrp-1 blocking experiments, soluble Nrp-1 (R&D Systems, 566-N1, 5 nM) or a Nrp-1–specific antibody (R&D Systems, AF566, 1 μg ml^{-1}) was added to the medium. Digital images were captured and analyzed using ImageJ software. Cell-free areas surrounding infected cells were measured (n = 10–26 cells per group).

Human genetics

Forty individuals with a primary or secondary diagnosis of PAPVC or TAPVC (21 individuals with PAPVC and 19 individuals with TAPVC) were ascertained through the Department of Cardiothoracic Surgery at the Children's Hospital of Philadelphia (CHOP) and voluntarily enrolled as part of a CHOP Institutional Review Board–approved protocol that included informed consent. PCR and sequencing primers were designed (using ExonPrimer, a Primer3-based algorithm available on the UCSC Genome Browser at http://genome.ucsc.edu/) for the coding and flanking intronic regions of *SEMA3D* on chromosome 7. The *SEMA3D* sequence annotation correlates to NM_152754. The primers were synthesized by Integrated DNA Technologies (http://www.idtdna.com) and reconstituted at 200 μM. Primer sequences, annealing temperatures and reaction conditions are available by request. PCR products were processed in the Nucleic Acids and Protein Core Facility at CHOP according to its standard Sanger sequencing protocols. Sequence analysis was carried out using both Sequencher v4.9 (Gene Codes Corporation, Ann Arbor, MI) and MacVector (MacVector, Inc.) software. All sequencing variants found were queried in the 1000 Genomes database (http://www.1000genomes.org/) and run through SIFT (http://sift.jcvi.org/) and PolyPhen v2 (http://genetics.bwh.harvard.edu/pph2/) to predict potential pathogenicity. Any variants not reported in the 1000 Genomes database were first confirmed in the affected individual and then tested in a cohort of 80 ethnically matched control samples. Because of the limited quantity of DNA available for each affected individual (<500 ng), a whole-genome amplification (WGA) reaction was required before PCR and sequencing. Briefly, 10 ng of each affected individual's DNA was used as template in the commercially available GenomiPhi V2 DNA Amplification kit (Illustra, Inc.), and each reaction was carried out according to the manufacturer's protocol. Agarose gel electrophoresis was used to assess the quality of the WGA DNA product. The final amplification product stocks for each affected individual were diluted 1:20 and stored at –20 °C for use in downstream PCR and sequencing reactions. The WGA DNA products were used as the template for all initial screening reactions of the *SEMA3D* coding sequence. After identification of a new coding variant in an affected individual's WGA DNA sequence, the PCR and sequencing reactions were repeated using 20 ng of the original stock DNA to confirm that the variant existed in the original DNA sample of the affected individual and was not introduced by the WGA reaction.

Statistical analyses

Two-tailed Student's *t* test or one-way ANOVA was used to analyze data. Significant differences calculated by ANOVA were further analyzed *post hoc* by Tukey's test for multiple comparisons (*$P < 0.05$, **$P < 0.01$, ***$P < 0.001$; NS, not significant). All data are expressed as the mean ± s.e.m.

Supplementary Material

Refer to Web version on PubMed Central for supplementary material.

Acknowledgments

We thank S.B. Bleyl for helpful comments and critical reading of the manuscript, N.A. Speck for technical assistance and B. Gelb and V. Garg for assistance with genetic analyses. This work was supported by US National Institutes of Health (NIH) grants NIH 5K12HD043245-07 (K.D.), NIH 5K08KL094763-02 (K.D.), NIH T32 GM07229 (H.A.) and NIH UO1 HL100405 (J.A.E.), the Spain Fund (J.A.E.) and the WW Smith Endowed Chair (J.A.E.).

References

1. Brody H. Drainage of the pulmonary veins into the right side of the heart. Arch. Pathol. (Chic). 1942; 33:221.
2. Lucas RV Jr. Amplatz K, Adams P Jr. Anderson RC, Edwards JE. Congenital causes of pulmonary venous obstruction. J. Pediatr. 1962; 61:281–282. [PubMed: 14467097]
3. Lucas RV Jr. Lock JE, Tandon R, Edwards JE. Gross and histologic anatomy of total anomalous pulmonary venous connections. Am. J. Cardiol. 1988; 62:292–300. [PubMed: 3041792]
4. Seale AN, et al. Total anomalous pulmonary venous connection: morphology and outcome from an international population-based study. Circulation. 2010; 122:2718–2726. [PubMed: 21135364]
5. Adachi, B. Das Venensystem der Japaner. 1st edn. Kenkyusha; Tokyo: 1933.
6. Healey JE Jr. An anatomic survey of anomalous pulmonary veins: their clinical significance. J. Thorac. Surg. 1952; 23:433–444. [PubMed: 14928263]
7. Hughes CW, Rumore PC. Anomalous pulmonary veins. Arch. Pathol. (Chic). 1944; 37:364–366.
8. Kalke BR, Carlson RG, Ferlic RM, Sellers RD, Lillehei CW. Partial anomalous pulmonary venous connections. Am. J. Cardiol. 1967; 20:91–101. [PubMed: 6026928]
9. Burroughs JT, Edwards JE. Total anomalous pulmonary venous connection. Am. Heart J. 1960; 59:913–931. [PubMed: 13806293]
10. Auer J. The development of the human pulmonary vein and its major variations. Anat. Rec. 1948; 101:581–594. [PubMed: 18882433]
11. Sizarov A, et al. Three-dimensional and molecular analysis of the arterial pole of the developing human heart. J. Anat. 2012; 220:336–349. [PubMed: 22296102]
12. DeRuiter MC, Gittenberger-De Groot AC, Wenink AC, Poelmann RE, Mentink MM. In normal development pulmonary veins are connected to the sinus venosus segment in the left atrium. Anat. Rec. 1995; 243:84–92. [PubMed: 8540635]
13. Douglas YL, Jongbloed MR, Deruiter MC, Gittenberger-de Groot AC. Normal and abnormal development of pulmonary veins: state of the art and correlation with clinical entities. Int. J. Cardiol. 2011; 147:13–24. [PubMed: 20674049]
14. Keane, JF.; Lock, JE.; Fyler, DC.; Nadas, AS. Nadas' Pediatric Cardiology. Saunders Elsevier; Philadelphia: 2006.
15. Moss, AJ.; Allen, HD. Moss and Adams' Heart Disease in Infants, Children, and Adolescents: Including the Fetus and Young Adult. Wolters Kluwer Health/Lippincott Williams & Wilkins; Philadelphia: 2008.
16. van den Berg G, Moorman AF. Development of the pulmonary vein and the systemic venous sinus: an interactive 3D overview. PLoS ONE. 2011; 6:e22055. [PubMed: 21779373]
17. Bleyl S, et al. A gene for familial total anomalous pulmonary venous return maps to chromosome 4p13-q12. Am. J. Hum. Genet. 1995; 56:408–415. [PubMed: 7847375]
18. Bleyl SB, et al. Analysis of a Scottish founder effect narrows the *TAPVR-1* gene interval to chromosome 4q12. Am. J. Med. Genet. A. 2006; 140:2368–2373. [PubMed: 17036341]
19. Bleyl SB, et al. Dysregulation of the *PDGFRA* gene causes inflow tract anomalies including TAPVR: integrating evidence from human genetics and model organisms. Hum. Mol. Genet. 2010; 19:1286–1301. [PubMed: 20071345]
20. Cinquetti R, et al. Transcriptional deregulation and a missense mutation define *ANKRD1* as a candidate gene for total anomalous pulmonary venous return. Hum. Mutat. 2008; 29:468–474. [PubMed: 18273862]
21. Kigel B, Varshavsky A, Kessler O, Neufeld G. Successful inhibition of tumor development by specific class-3 semaphorins is associated with expression of appropriate semaphorin receptors by tumor cells. PLoS ONE. 2008; 3:e3287. [PubMed: 18818766]
22. Kruger RP, Aurandt J, Guan KL. Semaphorins command cells to move. Nat. Rev. Mol. Cell Biol. 2005; 6:789–800. [PubMed: 16314868]
23. Larrivée B, Freitas C, Suchting S, Brunet I, Eichmann A. Guidance of vascular development: lessons from the nervous system. Circ. Res. 2009; 104:428–441. [PubMed: 19246687]

24. Gu C, et al. Semaphorin 3E and plexin-D1 control vascular pattern independently of neuropilins. Science. 2005; 307:265–268. [PubMed: 15550623]
25. Feiner L, et al. Targeted disruption of semaphorin 3C leads to persistent truncus arteriosus and aortic arch interruption. Development. 2001; 128:3061–3070. [PubMed: 11688556]
26. Berndt JD, Halloran MC. Semaphorin 3d promotes cell proliferation and neural crest cell development downstream of TCF in the zebrafish hindbrain. Development. 2006; 133:3983–3992. [PubMed: 16971468]
27. Sato M, Tsai HJ, Yost HJ. Semaphorin3D regulates invasion of cardiac neural crest cells into the primary heart field. Dev. Biol. 2006; 298:12–21. [PubMed: 16860789]
28. Katz TC, et al. Distinct compartments of the proepicardial organ give rise to coronary vascular endothelial cells. Dev. Cell. 2012; 22:639–650. [PubMed: 22421048]
29. Zhou Y, Gunput RA, Pasterkamp RJ. Semaphorin signaling: progress made and promises ahead. Trends Biochem. Sci. 2008; 33:161–170. [PubMed: 18374575]
30. Herzog Y, Guttmann-Raviv N, Neufeld G. Segregation of arterial and venous markers in subpopulations of blood islands before vessel formation. Dev. Dyn. 2005; 232:1047–1055. [PubMed: 15739224]
31. Pellet-Many C, et al. Neuropilin-1 mediates PDGF stimulation of vascular smooth muscle cell migration and signalling via p130Cas. Biochem. J. 2011; 435:609–618. [PubMed: 21306301]
32. Evans IM, et al. Neuropilin-1 signaling through p130Cas tyrosine phosphorylation is essential for growth factor–dependent migration of glioma and endothelial cells. Mol. Cell Biol. 2011; 31:1174–1185. [PubMed: 21245381]
33. Koppel AM, Feiner L, Kobayashi H, Raper JA. A 70 amino acid region within the semaphorin domain activates specific cellular response of semaphorin family members. Neuron. 1997; 19:531–537. [PubMed: 9331346]
34. Renzi MJ, Feiner L, Koppel AM, Raper JA. A dominant negative receptor for specific secreted semaphorins is generated by deleting an extracellular domain from neuropilin-1. J. Neurosci. 1999; 19:7870–7880. [PubMed: 10479689]
35. Fu W, et al. Analysis of 6,515 exomes reveals the recent origin of most human protein-coding variants. Nature. 2013; 493:216–220. [PubMed: 23201682]
36. Jiang Q, et al. Rapid and efficient human mutation detection using a bench-top next-generation DNA sequencer. Hum. Mutat. 2012; 33:281–289. [PubMed: 21898659]
37. Luzón-Toro B, et al. Mutational spectrum of Semaphorin 3A and Semaphorin 3D genes in Spanish Hirschsprung patients. PLoS ONE. 2013; 8:e54800. [PubMed: 23372769]
38. Chauvet S, et al. Gating of Sema3E/PlexinD1 signaling by neuropilin-1 switches axonal repulsion to attraction during brain development. Neuron. 2007; 56:807–822. [PubMed: 18054858]
39. Riccomagno MM, et al. The RacGAP β2-chimaerin selectively mediates axonal pruning in the hippocampus. Cell. 2012; 149:1594–1606. [PubMed: 22726444]
40. Silversides CK, et al. Rare copy number variations in adults with tetralogy of fallot implicate novel risk gene pathways. PLoS Genet. 2012; 8:e1002843. [PubMed: 22912587]
41. Katz TC, et al. Distinct compartments of the proepicardial organ give rise to coronary vascular endothelial cells. Dev. Cell. 2012; 22:639–650. [PubMed: 22421048]
42. Degenhardt K, Wright AC, Horng D, Padmanabhan A, Epstein JA. Rapid 3D phenotyping of cardiovascular development in mouse embryos by micro-CT with iodine staining. Circ. Cardiovasc. Imaging. 2010; 3:314–322. [PubMed: 20190279]
43. Yokomizo T, et al. Whole-mount three-dimensional imaging of internally localized immunostained cells within mouse embryos. Nat. Protoc. 2012; 7:421–431. [PubMed: 22322215]
44. Singh MK, Lu MM, Massera D, Epstein JA. MicroRNA-processing enzyme Dicer is required in epicardium for coronary vasculature development. J. Biol. Chem. 2011; 286:41036–41045. [PubMed: 21969379]
45. Merte J, et al. A forward genetic screen in mice identifies Sema3A(K108N), which binds to neuropilin-1 but cannot signal. J. Neurosci. 2010; 30:5767–5775. [PubMed: 20410128]
46. Gitler AD, Lu MM, Epstein JA. PlexinD1 and semaphorin signaling are required in endothelial cells for cardiovascular development. Dev. Cell. 2004; 7:107–116. [PubMed: 15239958]

47. Gu C, et al. Semaphorin 3E and plexin-D1 control vascular pattern independently of neuropilins. Science. 2005; 307:265–268. [PubMed: 15550623]

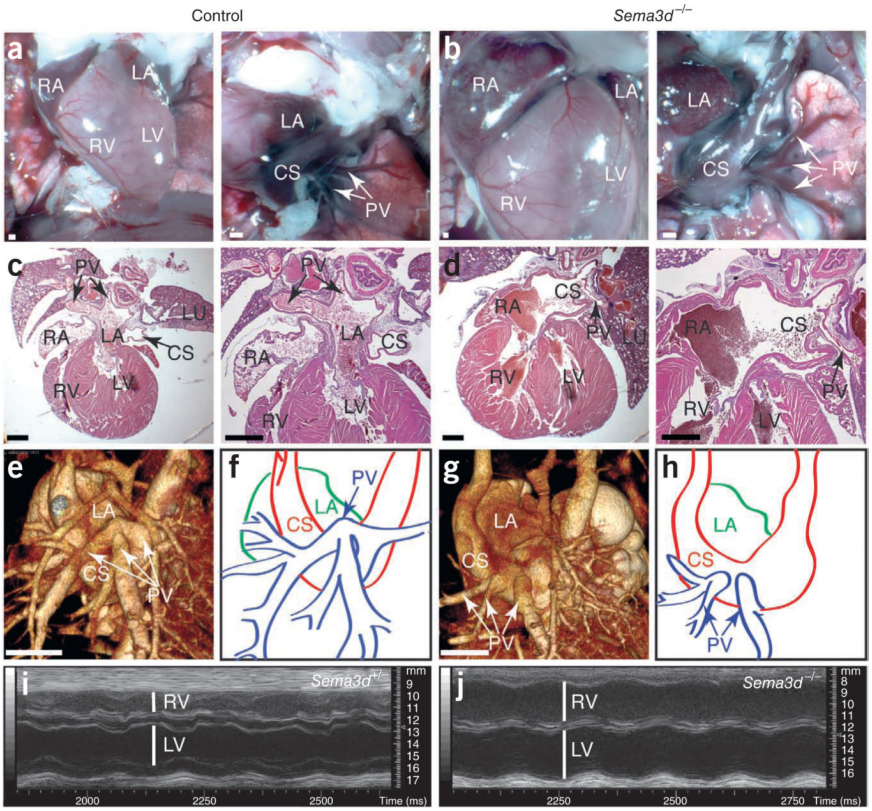

Figure 1.

Sema3d$^{-/-}$ mice have TAPVC. (**a,b**) Anterior views of adult control (**a**) and *Sema3d*$^{-/-}$ (**b**) hearts. *Sema3d*$^{-/-}$ showed severe cardiomegaly in the mutants due to right atrial (RA) and right ventricular (RV) dilation. Pulmonary veins (PV) enter the left atrium (LA) in the *Sema3d*$^{+/-}$ mouse (**a**, right) but enter the coronary sinus (CS) in the mutant mouse (**b**, right). (**c,d**) Photomicrographs of H&E-stained sections showing a normal connection of the pulmonary veins to the left atrium in *Sema3d*$^{+/-}$ mice (**c**) and anomalous pulmonary venous connections to the coronary sinus in *Sema3d*$^{-/-}$ mice (**d**). LU, lung. (**e–h**) Volume-rendered microcomputed tomography (microCT) images (dorsal view) showing the pulmonary veins entering the posterior left atrium in a newborn wild-type mouse (**e**) and entering the coronary sinus in a newborn mutant mouse (**g**). Also shown in **f** and **h** are diagrams of the microCT images in **e** and **g**, respectively. (**i,j**) M-mode echocardiograms through the ventricles of a *Sema3d*$^{+/-}$ (**i**) and a *Sema3d*$^{-/-}$ (**j**) heart showing the relative dilation of the right ventricle in an adult *Sema3d*$^{-/-}$ mouse as well as paradoxical septal wall motion indicative of right-sided volume overload. Scale bars (**a–e,g**), 1 mm.

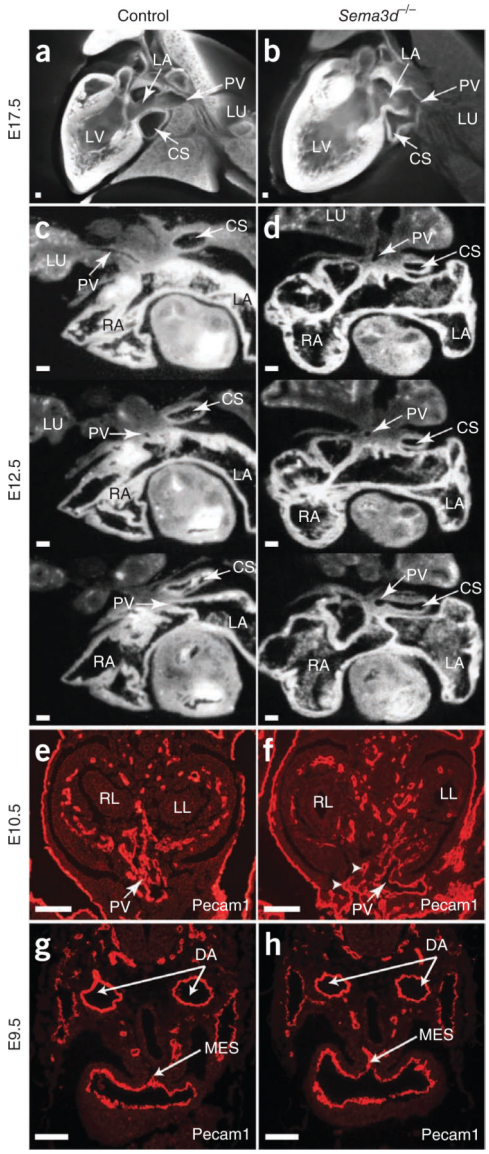

Figure 2.

Pulmonary vein patterning defects are present in *Sema3d*$^{-/-}$ embryos as early as E10.5. (**a,b**) Volume-rendered OPT images of late-stage (E17.5) wild-type (**a**) and *Sema3d*$^{-/-}$ (**b**) heart-lung tissue blocks. The wild-type sample shows a normal pulmonary vein connection to the left atrium, whereas the *Sema3d*$^{-/-}$ sample shows a connection to both the left atrium and coronary sinus. (**c,d**) Serial multiplanar reformatted OPT images of E12.5 wild-type (**c**) and *Sema3d*$^{-/-}$ (**d**) embryos, showing the course of the pulmonary vein from the lung to the left atrium in the wild-type sample and to the coronary sinus in the *Sema3d*$^{-/-}$ sample. See **Supplementary Video 3** for additional images. (**e,f**) Pecam1 immunofluorescence of E10.5 embryos. At this time point, the pulmonary vascular plexus coalesces into the pulmonary vein, which runs between the mesocardial folds. In the *Sema3d*$^{+/-}$ embryo (**e**), the pulmonary vein remains near the midline, whereas in the *Sema3d*$^{-/-}$ embryo, the pulmonary vein deviates laterally, and ectopic vessels (arrowheads) are present (**f**). (**g,h**) Pecam1 immunofluorescence at E9.5 showing no discernible abnormalities in a *Sema3d*$^{-/-}$ embryo (**h**) compared to a *Sema3d*$^{+/-}$ embryo (**g**). Notably, the MES forms normally in *Sema3d*$^{-/-}$

embryos (see **Supplementary Fig. 3** for images of **g** and **h** with adjacent sections). RL, right lung bud; LL, left lung bud; DA, dorsal aorta. Scale bars (**a–h**), 100 μm.

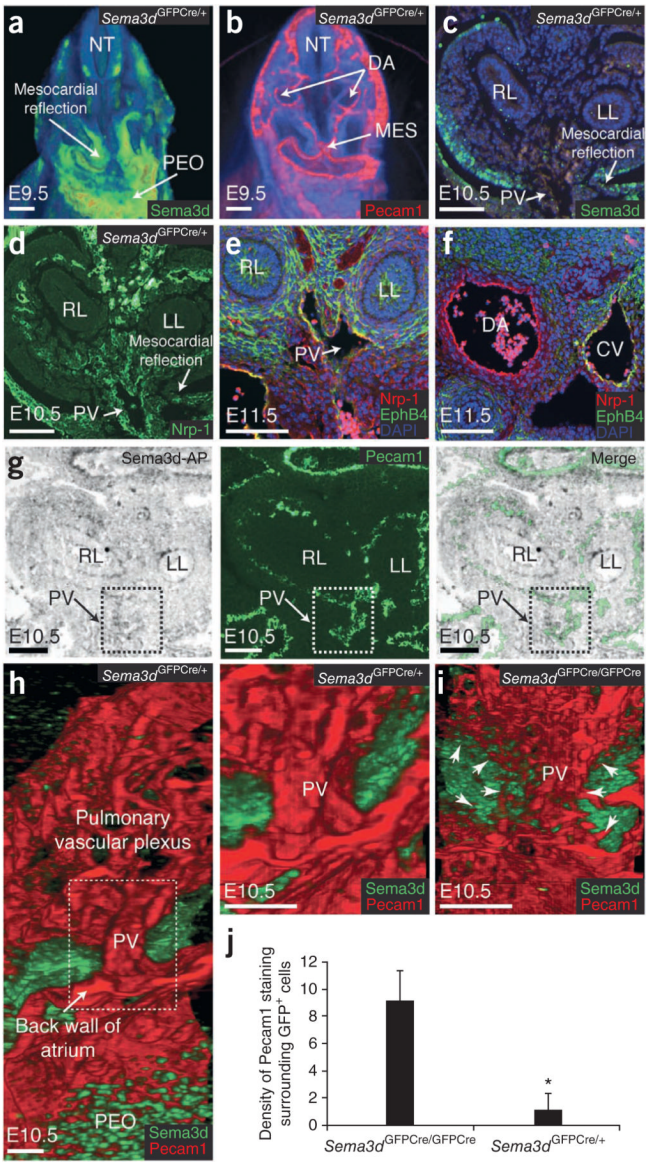

Figure 3.

Sema3d-expressing cells form a boundary that restricts the pulmonary endothelium. (**a**) Whole-mount GFP immunofluorescence in an E9.5 *Sema3d*$^{GFPCre/+}$ embryo viewed by OPT. Shown is a digitally-generated cross section of the three-dimensional volume-rendered image. Sema3d expression, marked by GFP (green), was observed in the mesocardial reflection and proepicardial organ (PEO). NT, neural tube. (**b**) Pecam1 immunofluorescence in an E9.5 *Sema3d*$^{GFPCre/+}$ embryo showing the MES in the same projection as **a**. (**c**) GFP immunofluorescence in an E10.5 *Sema3d*$^{GFPCre/+}$ embryo at the level of the pulmonary vein. (**d**) Adjacent section to **c** showing Nrp-1 immunofluorescence. (**e,f**) Coimmunofluorescence for Nrp-1 (red) and EphB4 (green) in an E11.5 embryo, showing that Nrp-1–expressing pulmonary vein endothelial cells also expressed EphB4 (**e**). Nrp-1 and EphB4 were coexpressed by endothelial cells of the cardinal veins (CV) but not of the dorsal aorta (**f**). (**g**) Sema3d-AP binding to transverse sections from an E10.5 embryo (left), Pecam1 immunofluorescence in an adjacent section (center), and the merged image (right). Boxes indicate an area of forming pulmonary veins. (**h,i**) Three-dimensional reconstruction

of confocal-imaged E10.5 *Sema3d*$^{GFPCre/+}$ (**h**) and *Sema3d*$^{GFPCre/GFPCre}$ (**i**) embryos stained for Pecam1 (red) and GFP (green). Shown are cross sections generated by digitally cutting the three-dimensional volume just above the pulmonary vein and then viewed from a cranial perspective. On the right in **h** is a close up of the boxed region in the image on the left. In (**i**), Pecam1-positive endothelial cells (arrows) intermingle with GFP-expressing cells. (**j**) Quantification of the density of Pecam1 staining within 10 μm of GFP-positive mesocardial cells in mutant (homozygous) and heterozygous embryos. $n = 4$; $^*P < 0.05$ (Student's *t* test). Data are shown as the mean ± s.e.m. Scale bars, 100 μm (**a–g**); 25 μm (**h,i**).

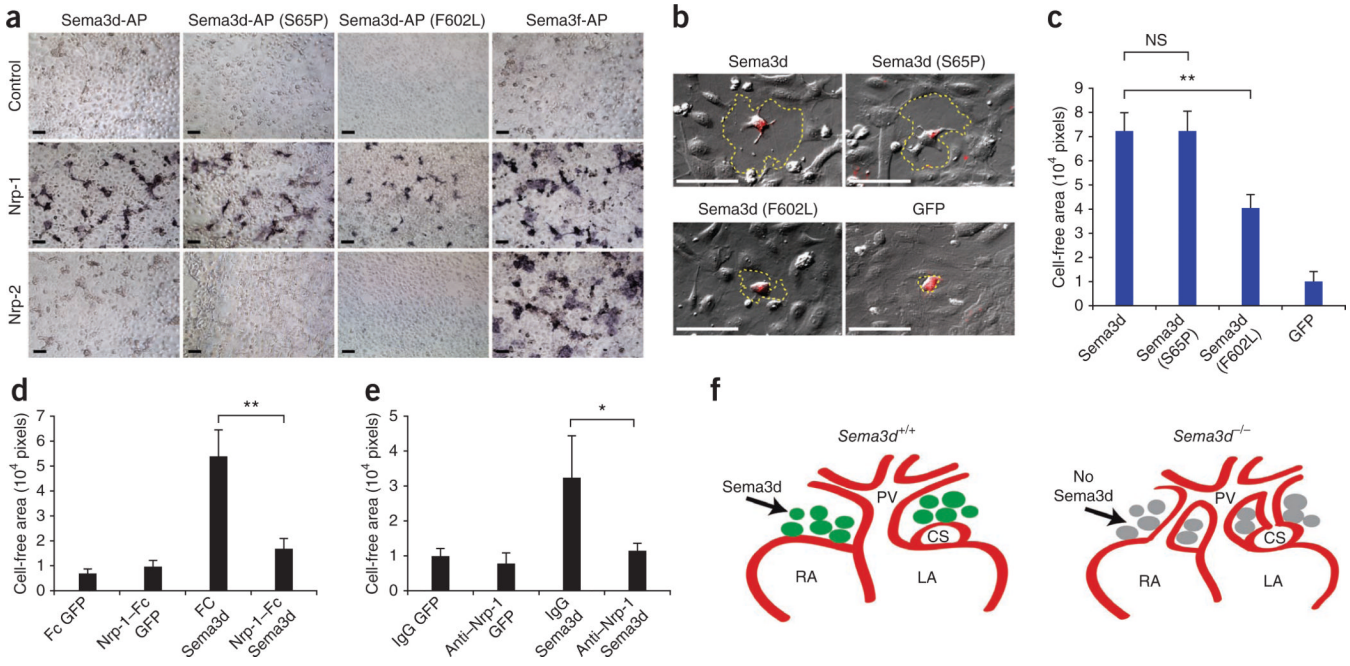

Figure 4.

Sema3d binds to Nrp-1 and is capable of repelling endothelial cells. (**a**) Representative photomicrographs showing binding of alkaline phosphatase fusion proteins containing wild-type or variant forms of Sema3d to control, Nrp-1–overexpressing or Nrp-2–overexpressing COS-7 cells. Sema3f-AP was included as a positive control that binds to both neuropilins. (**b**) Representative photomicrographs showing the repulsive effects of wild-type and variant forms of Sema3d on HUVECs. DiI-labeled (red) HEK293 cells transduced with Sema3d or control (GFP) lentivirus were cocultured with HUVECs. Repulsion of HUVECs results in a cell-free area (dashed yellow lines) surrounding the HEK293 cells. (**c**) Quantification of the cell-free area surrounding the HEK293 cells. ($n = 10$ per group; $P < 0.001$, one-way analysis of variance (ANOVA) between groups; *post-hoc* multiple comparisons, Tukey's test, $^{**}P < 0.01$). NS, not significant. (**d,e**) Effect of soluble Nrp-1 (Nrp-1–Fc) (5 nM) and an Nrp-1–specific blocking antibody (anti–Nrp-1) (1 μg ml^{-1}) on endothelial cell repulsion by HEK293 cells transduced with wild-type Sema3d or control lentivirus. Fc and IgG were used as controls. ($P < 0.01$, one-way ANOVA between groups; *post-hoc* multiple comparisons, Tukey's test, $^{*}P < 0.05$, $^{**}P < 0.01$). (**f**) Model showing the role of Sema3d in pulmonary vein patterning. Normally (left) Sema3d is expressed between the heart and the developing pulmonary vasculature where it repels endothelial cells to prevent the formation of anomalous connections. Deficiency of Sema3d (right) allows endothelial cells to enter this region and form anomalous vascular connections. $n = 10$ per group. Scale bars (**a,b**), 100 μm. Data (**c–e**) are shown as the mean ± s.e.m.